Anomalous scaling of nickel surfaces in pulse-current electrodeposition growth

M. Saitou

Department of Mechanical Systems Engineering, University of the Ryukyus, 1 Senbaru Nishihara-cho, Okinawa, 098-0213 Japan

(Received 13 February 2002; revised manuscript received 16 May 2002; published 29 August 2002)

We have made investigations into scaling properties of nickel surfaces grown by pulse-current electrodeposition using atomic force microscopy. The surface growth exhibits an anomalous dynamic scaling behavior characterized by a local roughness exponent $\zeta_{\rm loc}$, global scaling exponent ζ, and dynamic exponent z for an intermediate time regime $l^z \ll t \ll L^z$ where l and L denote a window length and system size. The local interface width of the nickel surfaces leads to $\zeta_{\rm loc}=1.0$, global scaling exponent $\zeta=2.8$ and dynamic exponent $z=4.1$. All the experimental data collapse on a plot of the anomalous scaling function proposed by López *et al.* [Phys. Rev. E **56**, 3993 (1997)].

DOI: 10.1103/PhysRevB.66.073416 PACS number(s): 68.55.Jk, 05.40.−a, 81.15.Pq

Kinetic surface roughening, far from equilibrium has been a study of great interest for the past decade.[1–3] Stochastic differential equations for growth have achieved explosive developments after Kadar *et al.*[4] proposed their nonlinear equation. Surface roughening in growth has been shown to exhibit scaling properties characterized by some scaling exponents that enable us to understand similar behaviors independent of specified systems.[5–11] The surface height $h(r,t)$ is statistically invariant under a self-affine transformation $h(r,t) \rightarrow \lambda^{-\alpha} h(\alpha r,t)$ where λ is an arbitrary constant and α is the roughness exponent that characterizes the roughness of saturated surfaces. The interface width that is the root mean square of the fluctuations of the surface height is defined by $W(L,t)=\langle [h(r,t)-\bar{h}]^2 \rangle^{1/2}$ where $\langle \cdots \rangle$ indicates an average over a system size L and $\bar{h}$ indicates an average of $h(r,t)$. The interface width obeys the Family-Vicsek function[1]

$$W(L,t)=t^{\alpha/z} f(L/t^{1/z}) \tag{1}$$

which behaves as

$$f(u) \sim \begin{cases} u^{\alpha} & \text{if } u \ll 1, \\ \text{const} & \text{if } u \gg 1, \end{cases} \tag{2}$$

where z is the dynamic exponent. The growth exponent β is given by $\beta=\alpha/z$, which represents the time-dependent dynamics of the surface roughness. These exponents α, β, and z determine the universality class which a system belongs to. Equation (1) indicates the presence of a saturation time t_s. The horizontal correlation length $\xi(t)$ is related to the saturation time t_s as $\xi(t) \sim t_s^{1/z}$. A great number of experiments on thin films grown by molecular beam epitaxy (MBE),[5,6] sputtering,[7,8] and electrodeposition[10,11] support the scaling behaviors described by the Family-Vicsek function.

However, recently it has been found that surface roughening in some theoretical models,[12–15] experiments of fracture surfaces,[16,17] and thin film surfaces in growth[18–20] deviate from the Family-Vicsek function. In Ref. 13, it is pointed out that anomalous scaling behaviors, for example, the growth exponent $\beta > 1/2$ may take place in electrochemical deposition. The value of β expected in the case of normal scaling is 0.5 and under. In fact, some experiments on electrodeposition[21,22] support the prediction. An anomalous scaling function related to a local interface width is proposed to describe the anomalous scaling behavior.[12] The local interface width $w(l,t)$ is defined by

$$w(l,t) \sim \begin{cases} t^{\beta_*} l^{\zeta_{\rm loc}} & \text{if } l^z \ll t \ll L^z, \\ t^{\zeta/z} & \text{if } t \ll l^z, \end{cases} \tag{3}$$

where $\beta_* = (\zeta - \zeta_{\rm loc})/z$ is an anomalous growth exponent and l is a window size. The local interface width $w(l,t)$ is calculated over a window size of l less than the system size L. Equation (3) indicates the presence of a crossover time for the time regime $l_z \ll t \ll L^z$ and the same form as the Family-Vicsek function for the time regime $t \ll l^z$. Hence the anomalous scaling system described by Eq. (3) has two roughness exponents: the local roughness $\zeta_{\rm loc}$ independent of experimental conditions and global roughness exponent ζ dependent on experimental conditions. For example, in Ref. 20, it was shown that in direct-current electrodeposition of copper, two exponents have constant values independent of experimental conditions $\zeta_{\rm loc}=0.77$ and $z=2.0$, and that the global roughness exponent ζ has a value ranging from 0.75 to 1.55 (these values are estimated from their experimental results). In other experiments that have reported the anomalous scaling behaviors,[16,17,23] it is recognized that the local roughness exponent $\zeta_{\rm loc}$ is insensitive to experimental conditions and the global roughness exponent ζ has a value dependent on experimental conditions.

Thin films electrodeposited on smooth substrates generally comprise a set of continuous mounds. The correlated length $\xi(t)$ is considered to be approximately equal to the mean diameter of the mound.[19] Pulse-current electrodeposition makes it possible that much smaller mounds grow on substrates in comparison with direct-current electrodeposition.[24] This is due to an enhancement of nucleation by the high pulse-current density that allows growth on sites where mounds are inhibited for direct-current electrodeposition. Hence, in pulse-current electrodeposition a cross-over time is expected to appear in the experimental time regime because of the saturation time $t_s \sim \xi^z$. In this study, nickel thin films by the pulse-current technique were grown on ITO (indium tin oxide coated) glasses for 50–2600

 ©2002 The American Physical Society

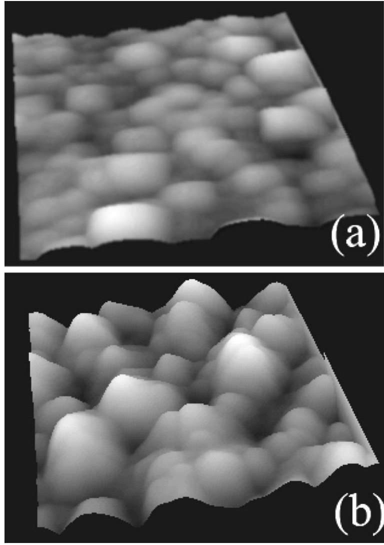

FIG. 1. AFM images of 1000×1000 nm^2 nickel surfaces at two different growth time: (a) $t=400$ sec and maximum $h(r,t)=106$ nm and (b) $t=2600$ sec and maximum $h(r,t)=182$ nm.

sec. Atomic force microscopy (AFM) was employed to characterize the surface morphology of the nickel deposits.

The purpose of this paper is to present the scaling behavior of surface roughening in pulse-current nickel electrodeposition that obeys the anomalous scaling function and to discuss the values of the local and global roughness exponents in electrodeposition. The experimental procedure for pulse-current electrodeposition was as follows. ITO glass substrates (sheet resistivity $6\Omega/\Box$) with a r.m.s. roughness of 1.2 nm cleaned by a wet process were prepared for both cathode and anode electrodes. The r.m.s. roughness of the ITO glass is too small to affect the roughness of nickel surfaces grown in this experiment. The two ITO glass substrates were located parallel in a still bath containing (g/l): nickel sulfamate, 600; nickel chloride, 5; and boric acid, 40. The bath was maintained at pH 4 and the temperature of 323 K. A square wave current pulse was applied between the two ITO electrodes. The current on-time and off-time were 2 and 8 msec, and the peak current density was 10 mA/cm^2, which were chosen based on the response rate of the system. The current off-time denotes the time interval at which no current supplies between the two ITO glasses. The average current density in pulse-current electrodeposition was 2 mA/cm^2. Nickel ions were electrodeposited on the ITO glass of 1×1 cm^2. The system size L in this experiment is 1 cm. The nickel thin films on the ITO glasses were grown for the growth time ranging from 50 to 2600 sec. The nickel deposits were scanned in air with AFM that has a resolution of 512×512 pixels. The Si_3N_4 cantilever used in this study has a tip radius less than 15 nm, which gives a high resolution enough to observe nickel mounds formed on the ITO glasses. The AFM images with different scan regions of 250×250, 500×500, 750×750 and 1000×1000 nm^2 were used for the calculations of the scaling exponents.

Figure 1 shows typical AFM images of nickel electrodeposits that comprise a set of continuous mounds. It can be seen that some mounds in Fig. 1(b) have cusps like pyramids. The film thickness of the electrodeposit at 100 sec was about 35 nm and the interface width was $w=3.7$ nm. The electrodeposit at 2600 sec reached a film thickness of 910 nm with $w=34$ nm. In comparison with the typical experimental result of $w=0.88$ nm at $h=37$ nm in MBE,[18] the surface of the electrodeposit is very rough, which allows us to determine the roughness exponent. The local roughness exponent $\zeta_{\rm loc}$ is determined by two methods: the Hurst rescaled range (R/S) analysis[25] and the Fourier transformation method.[26]

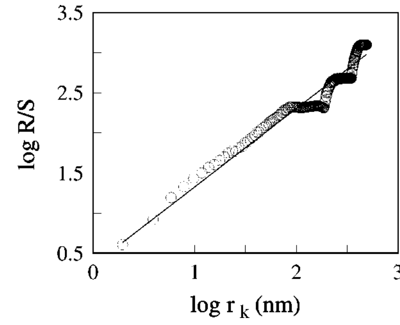

FIG. 2. Log-log plot of $R(k,t)/S(k,t)$ vs r_k calculated from the AFM images of 1000×1000 nm^2 electrodeposited for 1600 sec. The straight solid line that is best fitted to the data has a slope of 0.97.

The formula for the calculation of the exponent $\zeta_{\rm loc}$ in the R/S analysis is as follows: An arbitrary radius on the AFM images is represented by r_k:

$$R(k,t)/S(k,t)\sim r_k^{-\zeta_{\rm loc}}, \tag{4}$$

where

$$R(k,t)=\max_{0\leq i\leq k}[X(i,t)]-\min_{0\leq i\leq k}[X(i,t)], \tag{5a}$$

$$S(k,t)=\left[k^{-1}\sum_{i=1}^{k}[h(r_i,t)-\langle h(r,t)\rangle_i]^2\right]^{1/2}, \tag{5b}$$

$$X(k,t)=\sum_{i=1}^{k}[h(r_i,t)-\langle h(r,t)\rangle_k]. \tag{5c}$$

The value of $\langle h(r,t)\rangle_k$ denotes an average over the range of r_k beginning at r_1. The index k indicates a number that represents $r_1<r_2<\cdots<r_k$. First, we calculate $X(k,t)$ within a radius r_k on the AFM image. Next, we find the maximum and minimum change of $X(k,t)$ and normalize $R(k,t)$ by the standard deviation $S(k,t)$. Figure 2 shows a log-log plot of $R(k,t)/S(k,t)$ vs r_k for the AFM image of 1000×1000 nm^2 electrodeposited for 1600 sec. The slope of the best straight-fitted line to the data in Fig. 2 gives the local roughness exponent $\zeta_{\rm loc}=0.97$. The average $\zeta_{\rm loc}$ for the nickel films grown for 50–2600 sec becomes 1.00 ± 0.05.

On the other hand, the Fourier transformation method[26] is to determine the local roughness exponent $\zeta_{\rm loc}$ from the power spectrum. The power spectrum of $H(f,t)$ that is the Fourier transform of $h(r,t)$ is given by

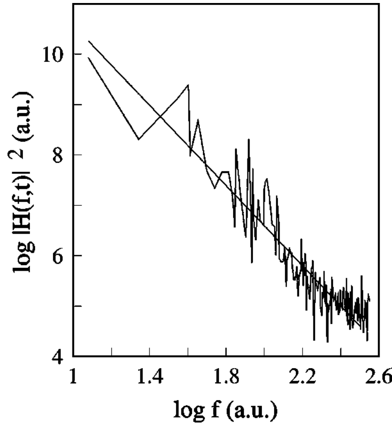

FIG. 3. Log-log plot of $|H(f,t)|^2$ vs f calculated from the AFM images of $1000\times1000\ \mathrm{nm}^2$ electrodeposited for 1600 sec. The straight solid line that is best fitted to the data has a slope of -3.98.

$$H(f,t)\sim f^{-\gamma}, \tag{6}$$

where f is the frequency and γ is a constant value. The local roughness exponent is expressed by the slope γ,

$$\zeta_{\mathrm{loc}}=(\gamma-2)/2. \tag{7}$$

Figure 3 shows a typical log-log plot of $|H(f,t)|^2$ vs the frequency f calculated from the same image used in Fig. 2. The slope of γ best fitted to the data yields 3.98. The average value of ζ_{loc} for the AFM images of the nickel surfaces grown by pulse-current electrodeposition becomes 1.00 ± 0.06, which is independent of the window length l. It is concluded that the local roughness ζ_{loc} obtained from the two methods is 1.0.

In order to prove the existence of an anomalous scaling behavior in this experiment, we need to indicate an anomalous exponent $\beta_*\neq0$. As the window length l decreases, if anomalous scaling takes place in pulse-current electrodeposition, the anomalous growth exponent β_* is expected to appear in a plot of $w(l,t)$ vs t in a log-log scale. Figure 4(a) shows the presence of a crossover time for the window size $l=500$ nm, which is in agreement with the anomalous scaling function of Eq. (3). In Fig. 4(a), ζ/z for the time regime $t\ll l^z$ and β_* for $l^z\ll t\ll L^z$, which are best fitted to the data, are estimated at 0.67 and 0.43. In Fig. 4(b), the slope of 0.67 for $t\ll l^z$, which is best fitted to the data corresponds to ζ/z. Using the values of the slopes, the global roughness exponent ζ and the dynamical exponent z are determined as 2.8 and 4.1. The local roughness exponent and dynamical exponent are very different from $\zeta_{\mathrm{loc}}=0.78$ and $z=2.0$ in the direct-current electrodeposition of copper[20] owing to the different growth mechanism. For example, no cusp structures are observed in the electrodeposited copper surfaces. But as shown in Fig. 1(b), the cusp structures of mounds seems to exist in pulse-current nickel electrodeposition. In nickel electrodeposition, the presence of preferential growth directions is generally recognized.[22] In Ref. 27, it was reported that calculations of the stochastic differential equation that describes the growth of pyramidlike mounds (surrounded by specific crystallographic planes) yield $\alpha=1.0$ and $z=4$. On

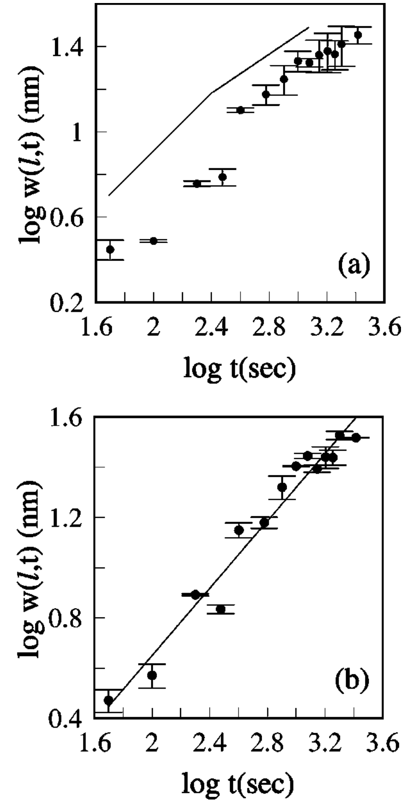

FIG. 4. Local interface width $w(l,t)$ vs t in a log-log scale for two different window lengths. The straight lines are shown to guide the eye. (a) For the window length l of 500 nm, there appears to be a time crossover. In the time regime $t\ll l^z$, the slope is 0.67 and in the time regime $l^z\ll t\ll L^z$, the slope is 0.43. (b) For the window length l of 1000 nm, the slope in the time regime $t\ll l^z$ is 0.67.

the other hand, in surface dimension $d=1$, numerical simulations of the linear surface diffusion model described by $\partial h(r,t)/\partial t=-K\nabla^4 h(r,t)+\eta(r,t)$ where $\eta(r,t)$ denotes the random fluctuation in deposition and K is constant give $\zeta_{\mathrm{loc}}=1.0$ and $z=4$.[12] These studies suggest that the nickel growth in pulse-current electrodeposition should be interpreted in view of surface diffusion and preferential growth of crystallographic planes.

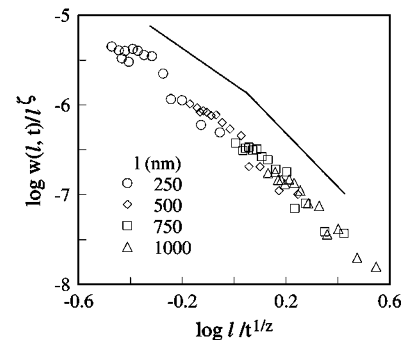

FIG. 5. The data collapse of the anomalous scaling function for window lengths $l=250$, 500, 750, and 1000 nm. The straight lines are plotted as a guide to the eye. The slopes for $u\ll1$ and $u\gg1$ are estimated at -2.8 and -1.8.

According to Ref. 12, the anomalous scaling function $g(l/t^{1/z}) = w(l,t)/l^{\zeta}$ is given from Eq. (3) as

$$g(u) \sim \begin{cases} u^{-(\zeta - \zeta_{\rm loc})} & \text{if } u \ll 1, \\ u^{-\zeta} & \text{if } u \gg 1. \end{cases} \tag{8}$$

Figure 5 shows that all the experimental data collapse on the anomalous scaling function represented by Eq. (8). The anomalous scaling function well describes the experimental results. The two straight lines for the time regimes $l/t^{1/z} \ll 1$ and $l/t^{1/z} \gg 1$ give a slope of -1.8 and -2.8. These values are consistent with $\zeta = 2.8$ and $\zeta_{\rm loc} = 1.0$ obtained from Eq. (3).

On the basis of anomalous scaling, surface roughening in pulse-current electrodeposition growth were examined using AFM. The presence of a crossover time for the experimental time regime is shown and the anomalous scaling exponents are determined as the local roughness exponent $\zeta_{\rm loc} = 1.0$, global roughness exponent$=2.8$, and dynamical exponent $z = 4.1$. All the data collapse on the anomalous scaling function, which indicates that the experimental results obey the anomalous scaling function.

This work was supported by Grant-in-Aid for Scientific Research (C), Grant No. 13650029 by the Ministry of Education, Science, and Culture of Japan.

[1] F. Family and T. Vicsek, *Dynamics of Fractal Surfaces* (World Scientific, Singapore, 1991).

[2] A. L. Barabási and H. E. Stanley, *Fractal Concepts in Surface Growth* (Cambridge University Press, Cambridge, England, 1995).

[3] A. C. Levi and M. Kotrla, J. Phys. C **9**, 299 (1997).

[4] M. Kadar, G. Paris, and Y. Zhang, Phys. Rev. Lett. **56**, 889 (1986).

[5] H. J. Ernst, F. Fabre, R. Folkerts, and J. Lapujoulade, Phys. Rev. Lett. **72**, 112 (1994).

[6] B. Reinker, M. Morske, and K. Samwer, Phys. Rev. B **56**, 9887 (1997).

[7] M. Lütt, J. P. Schlomka, M. Tolan, J. Stettner, O. H. Seeck, and W. Press, Phys. Rev. B **56**, 4085 (1997).

[8] H. You, R. P. Chiarello, H. K. Kim, and K. G. Vandervoort, Phys. Rev. Lett. **70**, 2900 (1993).

[9] D. M. Tanenbaum, A. L. Laracuente, and A. Gallagher, Phys. Rev. B **56**, 4243 (1997).

[10] J. Vázquez, R. C. Salvarezza, and A. J. Arvia, Phys. Rev. Lett. **79**, 709 (1997).

[11] B. E. Roberds and S. N. Farrens, J. Electrochem. Soc. **143**, 2365 (1996).

[12] J. M. López, M. A. Rodríguez, and R. Cuerno, Phys. Rev. E **56**, 3993 (1997).

[13] M. Castro, R. Cuerno, A. Sánchez, and F. D-Adame, Phys. Rev. E **57**, R2491 (1998).

[14] J. M. Ramasco, J. M. López, and M. A. Rodríguez, Phys. Rev. Lett. **84**, 2199 (2000).

[15] N. Pand and W. Tzeng, Phys. Rev. E **61**, 3559 (2000).

[16] J. M. López and J. Scmittbuhl, Phys. Rev. E **57**, 6405 (1998).

[17] S. Morel, J. Schmittbuhl, J. M. López, and G. Valentin, Phys. Rev. E **58**, 6999 (1998).

[18] N. H. Yang, G. C. Wang, and T. M. Lu, Phys. Rev. Lett. **73**, 2348 (1994).

[19] J. H. Jeffries, J. K. Zuo, and M. M. Craig, Phys. Rev. Lett. **76**, 4931 (1996).

[20] S. Huo and W. Schwarzacher, Phys. Rev. Lett. **86**, 256 (2001).

[21] S. Mendez, G. Andreasen, P. Schilardi, M. Figueroa, L. Vázquez, R. C. Salvarezza, and A. J. Arvia, Langmuir **14**, 2515 (1998).

[22] M. Saitou, A. Makabe, and T. Tomoyose, Surf. Sci. **459**, L462 (2000).

[23] A. Brú, L. M. Pastor, I. Fernaud, I. Brú, S. Melle, and C. Berenguer, Phys. Rev. Lett. **81**, 4008 (1998).

[24] J. C. Puippe and N. Ibl, J. Appl. Electrochem. **10**, 775 (1980).

[25] J. Feder, *Fractals* (Plenum, New York, 1988).

[26] A. I. Oliva, E. Anguiano, J. L. Sacedón, and M. Aguilar, Phys. Rev. B **60**, 2720 (1999).

[27] M. Siegert and M. Plischke, Phys. Rev. Lett. **73**, 1517 (1994).